Structural Studies by Exciton Coupled Circular Dichroism over a Large Distance: Porphyrin Derivatives of Steroids, Dimeric Steroids, and Brevetoxin B[⊥]

Stefan Matile,[†] Nina Berova,[†] Koji Nakanishi,*[,†] Jörg Fleischhauer,[‡] and Robert W. Woody*[,§]

Contribution from the Department of Chemistry, Columbia University, New York, New York 10027, Institut für Organische Chemie, RWTH Aachen, 52074 Aachen, Germany, and Department of Biochemistry and Molecular Biology, Colorado State University, Fort Collins, Colorado 80523-1870

Received January 16, 1996[⊗]

Abstract: The present study (see ref 1) delineates the scope and limitations of porphyrin chromophores for structural studies by the exciton coupled circular dichroic (CD) method. A distance dependency of the porphyrin coupling was investigated in the range between 10 and 50 Å. Over short interchromophoric distances, significant changes in the conformational distribution introduced by the bulky porphyrin chromophores were observed. Over longer distances, the porphyrins showed ca. 10-fold sensitivity increase over commonly used chromophores, and an effective direction for the interacting porphyrin transition moments was assigned by comparison. Porphyrins at the termini of dimeric steroids and brevetoxin B exhibited exciton coupling over interchromophoric distances *up to 50 Å.* These results represent the porphyrins as promising reporter chromophores for extending the exciton coupled CD method to structural studies of biopolymers.

Introduction

The exciton coupled circular dichroic (CD) method is a versatile and sensitive method for determining the absolute stereochemistry of organic molecules in solution.[2] In this procedure, two or more chromophores are attached to functional groups of the molecule of interest. The interaction between the excited states of these chromophores in chiral environments gives rise to bisignate CD curves, i.e., CD with split Cotton effects. The signs and shapes of the characteristic CDs are determined by the absolute skewness of interacting chromophores and, for relatively weak interactions, the principle of pairwise additivity.[3] When the original substrate already contains a chromophore, the newly introduced chromophore may be selected so that its absorption maximum will be close to that of the preexisting chromophore. However, in most cases overlap between the substrate and introduced chromophores complicate analyses of the CD curves. In order to avoid such interactions, the concept of "red-shifted" chromophores was developed.[4] Recently we have examined new acylating chromophores with intense absorbance (ϵ 31 000−58 000) at longer wavelengths (360−410 nm). Their applications to natural products, such as taxinine (λ_{max} 262 nm) and chromomycin A_3 (λ_{max} 270 nm),[4c] provided exciton split bands free of overlapping effects, thus leading to unambiguous analysis of the couplets. The amplitudes of split Cotton effects are inversely proportional to the square of interchromophoric distance[5] and proportional to the square of extinction coefficients[6] of the coupled chromophores. Therefore, exciton coupling over a long distance can be achieved only with strongly absorbing chromophores. So far, the long distance effects have been examined with rigid homosteroid[7] and norsteroid[8] derivatives where the interacting transition moments of para-substituted benzoates attached to rings A and D with a C−C distance of 18 Å showed CD amplitudes or *A* values (distance between extrema of couplets in $\Delta\epsilon$) up to ca. 20. While a distance of 18 Å practically covers all common natural products, the moderate *A* value of ca. 20 observed for benzoate chromophores is insufficient when dealing with samples available only in minuscule amounts, or samples in which the distance between stereogenic centers is much longer. Consequently, chromophores with more intense absorptions therefore with increased sensitivities are needed.

Although the exciton coupled CD method has proved to be a sensitive tool in elucidating the absolute configuration and detection of even small conformational changes,[2] its applicability in structural studies of biopolymers such as proteins or nucleic

[†] Columbia University.
[‡] Institut for Organische Chemie.
[§] Colorado State University.
[⊥] Abbreviations: BTX: brevetoxin; DBU: 1,8-diazobicyclo[5.4.0]undec-7-ene; DDQ: 2,3-dichloro-5,6-dicyano-1,4-benzoquinone; DMAP: *N,N′*-dimethyl-4-aminopyridine; dmab: dimethylaminobenzoate; DPMS: diphenylmethylsilyl; EDC: 1-(3-dimethylaminopropyl)-3-ethylcarbodiimide; TBA: tetrabutylammonium.
[⊗] Abstract published in *Advance ACS Abstracts,* May 15, 1996.

(1) Matile, S.; Berova, N.; Nakanishi, K.; Novkova, S.; Philipova, I.; Blagoev, B. *J. Am. Chem. Soc.* **1995**, *117*, 7021.
(2) (a) Harada, N.; Nakanishi, K. *Circular Dichroic Spectroscopy-Exciton Coupling in Organic Stereochemistry*; University Science Books: Mill Valley, CA, 1983. (b) Nakanishi, K.; Berova, N. In *Circular Dichroism-Principles and Applications*; Nakanishi, K., Berova, N., Woody, R. W., Eds.; VCH Publishers, Inc.: New York, NY, 1994; p 361.
(3) (a) Liu, H. W.; Nakanishi, K. *J. Am. Chem. Soc.* **1981**, *103*, 5591. (b) Wiesler, W. T.; Vazquez, J. T.; Nakanishi K. *J. Am. Chem. Soc.* **1987**, *109*, 5586. (c) Wiesler, W. T.; Berova, N.; Ojika, M.; Meyers, H. V.; Chang, M.; Zhou, P.; Lo, L.-C.; Niwa, M.; Takeda, R.; Nakanishi, K. *Helv. Chim. Acta* **1990**, *73*, 509.
(4) (a) Verdine, G. L.; Nakanishi, K. *J. Chem. Soc., Chem. Commun.* **1985**, 1093. (b) Berova, N.; Gargiulo, D.; Derguini, F.; Nakanishi, K.; Harada, N. *J. Am. Chem. Soc.* **1993**, *115*, 4769. (c) Cai, G.; Bozhkova, N.; Odingo, J.; Berova, N.; Nakanishi, K. *J. Am. Chem. Soc.* **1993**, *115*, 7192. (d) Gargiulo, D.; Ikemoto, N.; Odingo, J.; Bozhkova, N.; Iwashita, T.; Berova, N.; Nakanishi, K. *J. Am. Chem. Soc.* **1994**, *116*, 3760.
(5) Harada, N.; Chen, S.-M. L.; Nakanishi, K. *J. Am. Chem. Soc.* **1975**, *97*, 5345.
(6) Heyn, M. P. *J. Phys. Chem.* **1975**, *79*, 2424.
(7) Chen, S. L.; Harada, N.; Nakanishi, K. *J. Am. Chem. Soc.* **1974**, *96*, 7352.
(8) Canceill, J.; Collet, A.; Jacques, J. *J. Chem. Soc., Perkin II* **1982**, 83.

S0002-7863(96)00126-6 CCC: $12.00

acids with covalently attached reporter chromophores has not been explored. One obstacle was the strong interfering absorption of the biopolymers themselves below ca. 300 nm, which therefore required suitable CD chromophores with an absorption above 400 nm. More importantly, the distances encountered in biopolymers need a CD chromophore which can couple over a long distance, namely, a chromophore with a very high extinction coefficient. The cyanine dye chromophores exhibit intense, red-shifted absorptions around 520 nm with narrow half-band widths of 1520 cm^{-1}; however, chemical instability makes them unsuited for practical applications.[4b]

The porphyrin chromophore, i.e., 5-substituted 5,10,15,20-tetraphenylporphyrins, e.g., **1**, was therefore investigated.[1] With their very intense, sharp Soret band at 414 nm, ϵ 350 000,[9] they should provide powerful CD chromophores for configurational and conformational analysis of natural products with remote stereogenic centers and for conformational studies of biopolymers.

Analyses of CD of porphyrin monomers induced by proteins[10] or nucleic acids[11] is a well established procedure to investigate complex formation. The importance of this analytical technique has led to model CD studies of oligopeptides covalently linked to a porphyrin monomer.[12] Investigations of heme/heme interactions in multiheme proteins by CD are complicated by effects induced by amino acids surrounding each porphyrin chromophore. However, comparison of CD spectra of mono- and multiheme proteins suggested heme/heme interactions; calculations based on coordinates of isolated heme moieties taken from protein X-ray structures confirmed the possibility of long distance heme/heme interaction.[13] The unique physical properties of the photosynthetic reaction center gave rise to the synthesis of several model compounds, i.e., aryl- and alkyl-bridged porphyrin dimers.[14] Shifts and/or splitting of the Soret band in the UV−vis spectra of such achiral bridged porphyrin dimers have been attributed to exciton coupling strongly dependent on angle and distance. Chlorophyll dimers[15] and a dipeptide-bridged porphyrin dimer[16] exhibit exciton coupled Cotton effects in the CD. However, the nature of the observed CD remained obscure, because the effects of mono-and asymmetric disubstitution on the magnitude and direction of the Soret transition moments have been uncertain.[17] The effects of substitution by one or two vinyl or formyl groups have been clarified by recent theoretical studies.[18]

The Soret band consists of two perpendicularly polarized transitions, B_x and B_y (Figure 1A). In symmetrically substituted metalloporphyrins, which have fourfold symmetry, these transitions are degenerate and have identical intensities. In the free-base form of the porphyrin, with their lower symmetry, these transitions are not exactly degenerate and they will in general differ in intensity. However, most experimental and theoretical evidence argues against any sizable splitting or intensity difference in the components of the Soret band. Rimington et al.[19a] found a splitting of 250 cm^{-1} in the Soret band of free-base porphin at low temperatures. Polarized reflection spectra[19b] of porphin single crystals show different polarization on the long-wavelength and short-wavelength sides of the Soret maximum, but these data have not been analyzed quantitatively, so the extent of the splitting and the imbalance in oscillator strengths is not known. The spectrum of the free-base form of TPP is very similar to that of the Zn complex in the Soret transition, except for a shift in λ_{max}, some broadening and a concomitant decrease in ϵ_{max} in the free-base form. In particular, there is no detectable splitting of the strong major peak in the free-base form, and both forms show the shoulder about 1200 cm^{-1} above the main peak. It is well-known that free-base porphyrins show strong splitting of the visible (Q) bands, but as pointed out by Gouterman[20] this does not necessarily imply a substantial deviation from fourfold symmetry. Explicit MO calculations on free-base porphin give splittings of 25−250 cm^{-1} for the B_x and B_y bands, depending on the parameters. These calculations also predicted similar intensities of the B_x and B_y bands, with the ratio of transition moments predicted to range from 1.03 to 1.16. Recently, further semiempirical MO calculations on porphin in its free-base and dianion form have been reported.[18] These calculations predict a rather different picture for free-base porphin, in which the two Soret components are split by 2100 cm^{-1} (30 nm) and the ratio of the transition moments is ca. 1.5. Although these calculations are more sophisticated and give predictions for the splitting between the Soret and the visible bands, the splitting of the *x* and *y* components of the Q band, and the intensities of the Q bands that agree better with experiment than the earlier calculations,[20,21] the results for the Soret band appear to be less satisfactory. First, if the splitting of the Soret components were as large as predicted, one should be able to see two Soret peaks, contrary to observation. Second, the calculations also predict bands that are about twice as intense as the Soret band in the 310−320 nm region, where the absorption is in fact quite weak.

(9) (a) Falk, J. E. *Porphyrins and Metalloporphyrins*; Elsevier: Amsterdam, 1964. (b) Gouterman, M. In *The Porphyrins Vol. 3, Physical Chemistry, Part A*; Dolphin, D., Ed.; Academic: New York, NY, 1978.

(10) (a) Beychok, S.; Blout, E. R. *J. Mol. Biol.* **1961**, *3*, 769. (b) T. Samejima, T.; Yang, J. T. *J. Mol. Biol.* **1964**, *8*, 863. (c) Urry, D. W. *J. Am. Chem. Soc.* **1967**, *89*, 4190. (d) Myer, Y. P. *Biochim. Biophys. Acta* **1970**, *214*, 94. (e) Sugita, Y.; Nagai, M.; Yoneyama, Y. *J. Biol. Chem.* **1971**, *246*, 383. (f) Hsu, M.-C.; Woody, R. W. *J. Am. Chem. Soc.* **1971**, *93*, 3515. (g) Keinan, E.; Benory, E.; Sinha-Bagchi, A.; Eren, D.; Eshar, Z.; Green, B. S. *Inorg. Chem.* **1992**, *31*, 5433. (h) Nezu, T.; Ikeda, S. *Bull. Chem. Soc. Jpn.* **1993**, *66*, 18. (i) Woody, R. W. in ref 2b; p 473.

(11) (a) Carvlin, M. J.; Fiel, R. *Nucl. Acid Res.* **1983**, *11*, 6121. (b) Carvlin, M. J.; Mark, E.; Fiel, R.; Howard, J. C. *Nucl. Acid Res.* **1983**, *11*, 6141. (c) Pasternack, R. F.; Garrity, P.; Ehrlich, B.; Davis, C. B.; Gibbs, E. J.; Orloff, G.; Giartosio, A.; Turano, C. *Nucl. Acid Res.* **1986**, *14*, 5919. (d) Gibbs, E. J.; Maurer, M. C.; Zhang, J. H.; Reiff, W. M.; Hill, D. R. F. *J. Inorg. Biochem.* **1988**, *32*, 39. (e) Foster, N.; Singhal, A. K.; Smith, M. W.; Marcos, N. G.; Schray, K. J. *Biochim. Biophys. Acta* **1988**, *950*, 118. (f) Marzili, L. G.; Pethö, G.; Lin, M.; Kim, M. S.; Dixon, D. W. *J. Am. Chem. Soc.* **1992**, *114*, 7575. (g) Pasternack, R. F.; Bustamante, C.; Collings, P. J.; Giannetto, A.; Gibbs, E. J. *J. Am. Chem. Soc.* **1993**, *115*, 5393. (h) Pethö, G.; Elliot, N. B.; Kim, M. S.; Lin, M.; Dixon, D. W.; Marzili, L. G. *J. Chem. Soc., Chem. Commun.* **1993**, 1547.

(12) (a) Nishino, N.; Mihara, H.; Hasegawa, R.; Yanai, T.; Fujimoto, T. *J. Chem. Soc., Chem. Commun.* **1992**, 692. (b) Mihara, H.; Nishino, N.; Hasegawa, R.; Fujimoto, T. *Chem. Lett.* **1992**, 1805.

(13) Woody, R. W. in *Optical Properties and Structure of Tetrapyrroles*; Blauer, G., Sund, H., Eds.; Walter de Gruyter & Co.: Berlin, 1985; p 239.

(14) (a) Osuka, A.; Maruyama, K. *J. Am. Chem. Soc.* **1988**, *110*, 4454. (b) Wasielewski, M. R. *Chem. Rev.* **1992**, *92*, 435.

(15) Bucks, R. R.; Boxer, S. G. *J. Am. Chem. Soc.* **1982**, *104*, 340.

(16) Tamiaki, H.; Suzuki, S.; Maruyama, K. *Bull. Chem. Soc. Jpn.* **1993**, *66*, 2633.

(17) Hsu and Woody[10f] inferred that the Soret components in myoglobin are polarized along the methine carbon axes (B_x', B_y' in Figure 1A) because this orientation gave the best agreement between theory and experiment for the shape of the Soret CD band. Similar considerations led Fuhrhop et al. (Fuhrhop, H.-J.; Demoulin, D.; Boettcher, C.; König, J.; Siggel, U. *J. Am. Chem. Soc.* **1992**, *114*, 4159) to the same assignment of transition moment directions in theoretical analyses of the CD spectra of self-assembled protoporphyrin IX 13,17-bis-(glucosamides). Osuka and Maruyama[14a] assumed a 5−15-direction of the Soret transition in a C(5)-substituted porphyrin and estimated its magnitude (footnote 10 in ref 14a). However, as noted in the text of this paper, the interpretation of the fine structure of the Soret band made in ref 14a is not correct.

(18) (a) Masthay, M. B.; Findsen, L. A.; Pierce, B. M.; Bocian, D. F.; Lindsey, J. S.; Birge, R. R. *J. Chem. Phys.* **1986**, *84*, 3901. (b) Bocian, D. F.; Masthay, M. B.; Birge, R. R. *Chem. Phys. Lett.* **1986**, *125*, 467.

(19) (a) Rimington, C.; Mason, S. F.; Kennard, O. *Spectrochim. Acta* **1958**, *12*, 65. (b) Anex, B. G.; Umans, R. S. *J. Am. Chem. Soc.* **1964**, *86*, 5026.

(20) Gouterman, M. *J. Chem. Phys.* **1959**, *30*, 1139.

(21) Weiss, C.; Kobayashi, H.; Gouterman, M. *J. Mol. Spectrosc.* **1965**, *16*, 415.

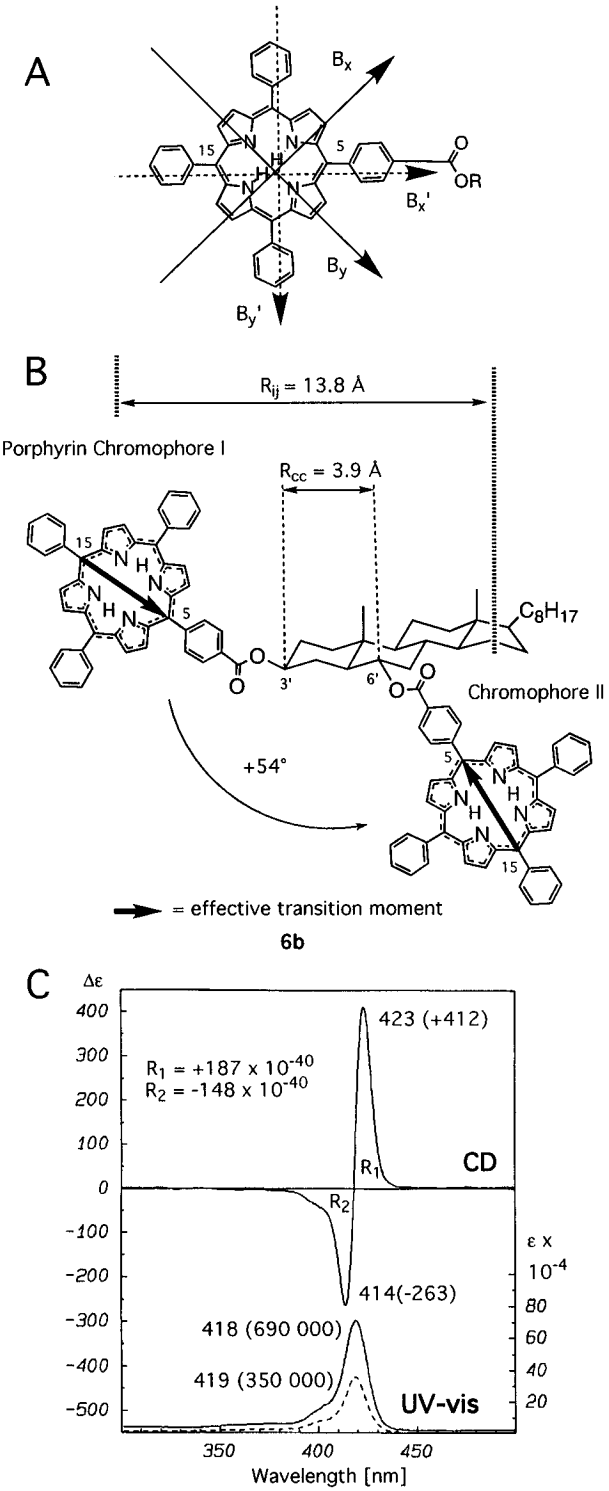

Figure 1. A: Two choices of transition moment directions for the porphyrin Soret transition. The directions labeled B_x and B_y are directed along the N−H/N−H and the N/N axes, respectively. However, because of the near degeneracy and approximate equivalence of these transitions, any linear combination of B_x and B_y can also be used. One such combination, designated B_x' and B_y', is shown as dashed lines and is directed between opposite methine carbons. B: Indication of the direction of the effective transition moment in **6b**. C: CD data of **6b** and UV−vis data of **6b** and **1** (dotted) in CH_2Cl_2, c = 1.0 μM. In all measured CD spectra no bands were detectable in the visible region above 500 nm, and the exciton CD spectra are only slightly altered when the free-base porphyrins are converted to the Zn complexes or are protonated, thus making them four-fold symmetric.

In light of this evidence, previous assignments of the main Soret absorption feature in tetraphenylporphyrins, near 420 nm, to the B_x transition and of the weak shoulder near 400 nm to the B_y transition are in error. The fine structure of the Soret band must instead be attributed to vibronic fine structure in the combined B_x, B_y bands: a 0 → 0 band near 420 nm and a 0 → 1 band near 400 nm. Thus, we cannot expect the porphyrin chromophore to behave like a linear oscillator as previously assumed. Instead, it must be treated as a nearly circular oscillator, with two nearly degenerate, orthogonal transition moments of approximately the same magnitude (Figure 1A). This implies that the simple exciton chirality method cannot be applied to these bisporphyrin systems. However, in all cases we have examined in which the bisporphyrin derivative can be compared with the bis(*p*-dimethylaminobenzoyl) derivative, the signs of the exciton effects are identical.[1] This suggests that an effective transition moment direction can be derived for these circular oscillators that gives the same sign as the normal exciton chirality rule for linear oscillators (Figure 1B). In addition, theoretical exciton calculations that include the doubly degenerate B_x and B_y transitions in each porphyrin have been performed for a number of conformers of **6b**−**9b** with dihedral angles at each stereogenic center varied about the minimum energy conformation deduced for benzoate esters.[2a,5] The four rotational strengths that result occur in pairs, corresponding to a strong inner couplet and a weak outer couplet, the latter generally opposite in sign to the former. In all cases, when Gaussian bands with the half bandwidth observed in the absorption spectrum are used to calculate the CD spectrum, a single couplet is predicted for the Soret region. Although individual conformers of a given isomer can vary in the sign of the predicted couplet, the sign of the unweighted average for each of the molecules **6b**−**9b** agrees with experiment, and the magnitude is in reasonable agreement. Further theoretical studies are in progress that will provide predicted CD spectra properly weighted by conformational energies and will further test the relationship between the correct B_x, B_y representation and the simplified model of one effective Soret transition moment per porphyrin.

Scheme 1

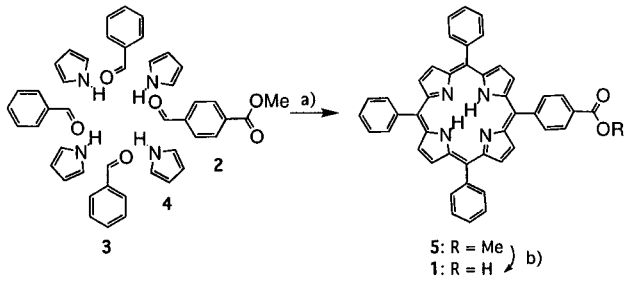

a) 1. $Zn(OAc)_2$, propionic acid, reflux, 4 h; 2. DDQ, pyridine, CH_2Cl_2, rt, 1 h; 3.18% aq. HCl/CH_2Cl_2 1:1, rt, 5 min, 7.5%; b) 2N aq. KOH/EtOH 1:10, reflux, 4 h, 86%.

Results and Discussion

Porphyrin Synthesis and Derivatization. Condensation of *p*-(carboxymethyl)benzaldehyde (**2**), benzaldehyde (**3**), and pyrrole (**4**) in propionic acid in the presence of zinc acetate,[22] followed by removal of zinc, gave ester **5**, which was hydrolyzed to porphyrin **1** in 6.5% overall yield (Scheme 1). Derivatization of all glycols (**6a**−**11a**) was performed under mild conditions—room temperature, overnight—in CH_2Cl_2/EDC/DMAP,[23] and afforded bisporphyrin derivatives **6b**−**11b** in 60−80% yield

(22) (a) Anton, J. A.; Loach, P. A. *J. Heterocyclic Chem.* **1975**, *12*, 573. (b) Stäubli, B.; Fretz, H.; Piantini, U.; Woggon, W.-D. *Helv. Chim. Acta* **1987**, *70*, 1173.

(23) Dhaon, M. K.; Olsen, R. K.; Ramasamy, K. *J. Org. Chem.* **1982**, *47*, 1962.

Table 1. CD Data of Bisporphyrins and Bis(*p*-dimethylaminobenzoates (dmab)) of Various Glycols, Measured at Concentrations between 0.8 and 1.2 μM

Chromophores	Glycols	Compounds	Solvents	R_{CC}[a]	R_{ji}[b]	1st λ(Δε)	2nd λ(Δε)	A
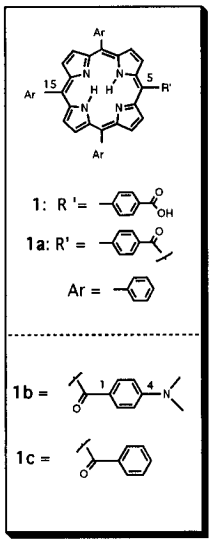		**12a**: R = H **12b**: R = **1a**	MeCN	1.2[c]	10[d]	421 (-230)	412(+170)	-400
	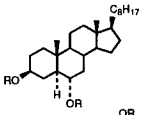	**6a**: R = H **6b**: R = **1a** **6c**: R = **1b**	CH_2Cl_2 CH_2Cl_2	3.9 3.9	13.0 5.0	423(+412) 319(-30)	414(-263) 294(-30)	+675[e] +89[e]
	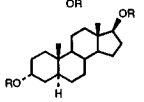	**7a**: R = H **7b**: R = **1a** **7c**: R = **1b**	CH_2Cl_2 20% Dioxane-EtOH	8.8 8.8	24.4 14.5	423(+111) 316(+17)	414(-77) 289(-4)	+188[e] +21[f]
	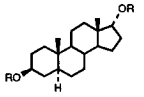	**8a**: R = H **8b**: R = **1a**	CH_2Cl_2	8.8	23.4	423(-61)	414(+48)	-109[e]
	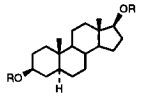	**9a**: R = H **9b**: R = **1a** **9c**: R = **1b** **9d**: R = **1c**	CH_2Cl_2 CH_2Cl_2 CH_2Cl_2	8.8 8.8 8.8	22.7 13.6 13.6	423(-12) 318(-3) 226(+3)	415(+21) 293(+5) --------	-32[e] -8[e] ----[e]
	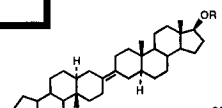	**10a**: R = H **10b**: R = **1a**	CH_2Cl_2	13.4	29.1	423(+10)	414(-1)	+11
	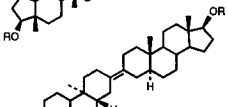	**11a**: R = H **11b**: R = **1a** **11c**: R = **1b**	CH_2Cl_2 CH_2Cl_2	18.3 18.3	34.0 25.0	423(+23) 311(+2)	414(-9) ---------	+32 -----
	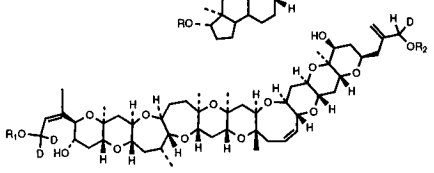	**13a**: $R_1 = R_2$ = H **13b**: $R_1 = R_2$ = **1a** **13c**: R_1 or R_2 = **1a**, R_1 or R_2 = H	H_2O/MeOH 1:4 H_2O/MeOH 1:4 + CsCl H_2O/MeOH 1:4	35[g] 35[g] ---	50[g] 50[g] ---	421(-6) 423(-8) ---------	406(+1) 406(+2.5) --------	-7 -10.5 -----

[a] Distance between the stereogenic centers, measured in a energy minimized structure (MacroModel 4.5).[37] [b] Distance between the chromophoric centers (see Figure 1B). [c] All distances are given in Å. [d] Due to the mixture of conformers, the average value is given. [e] Data already published in the preliminary communication.[1] [f] Data from ref 5. [g] Due to the semiflexibility of the brevetoxin bridge, the given distances will vary upon conformational changes.

(Table 1). The harsher conditions required to convert 1*R*,2*R*-cyclohexanediol (**12a**) as well as the lower yield (54%) of bisester **12b** can be explained by the conformational change of the cyclohexane ring which must precede the second esterification in order to minimize steric interaction of the porphyrin chromophores. Although the mono(**13c**)- and trisesters have been isolated, selective esterification of the allylic alcohols of the brevetoxin B derivative **13a** was already completed after 2 h giving bisporphyrin **13b** as the main product in 32% yield. Derivatization of steroids **7a**, **9a**, and **11a** with dimethylaminobenzoyl triazole/DBU[4d] gave bisester **7c**, **9c**, and **11c**. CD data are listed in Table 1.

13−24 Å Interchromophoric Distance. Conformational flexibility does not need to be considered when dealing with rigid steroid skeletons, which enable unambiguous investigations of distance and angle dependency of exciton coupled CD to be performed.[1,2,7] Of the known steroidal bis-chromophoric systems, 3,6-bis(dimethylaminobenzoate) **6c** exhibited the strongest coupling ($A = +89$) (Table 1).[7] Compared to **6c**, the CD of 3,6-bisporphyrin ester **6b** exhibited a bisignate CD with a >7-fold stronger amplitude of +675 (Figure 1C); however, this comparison is not a true measure of the increase in sensitivity, since despite the constant C−C distance of 3.9 Å between the chiral centers, the interchromophoric distance is 8 Å longer in bisporphyrin **6b** ($R_{ij} = 13.0$ Å) compared to bisbenzoate **6c** ($R_{ij} = 5.0$ Å).

Because of the known *syn* orientation of the ester carbonyl with respect to the methine hydrogen, the positive sign of the Cotton effect in **6c** reflects the chiral twist between the transition moments of dimethylaminobenzoate which lies in the direction of the phenyl 1,4-axis or the C(3)−O/C(6)−O bonds (Table 1). That the signs of the Cotton effects of bis(dimethylaminobenzoate) **6c** and bisporphyrin ester **6b** are the same indicate that the direction of the effective coupling transition moments of the porphyrins run in the same direction, i.e., 5,15-axis of the porphyrin ring, as shown in **6b**, Figure 1B; same is true for **7b**/**7c** and **9b**/**9c**. Therefore, the chiral sense of twist between the porphyrin chromophores attached to the stereogenic centers can be correctly simulated by the thick arrows depicted in structure **6b**, which in turn represents the chirality between the two C−O bonds in question as in the case of other symmetric chromophores, e.g., para-substituted benzoates.[24,25]

Comparisons of the bisporphyrin series **7b**, **8b**, and **9b**,

(24) The possibility exists that due to hydrophobic interactions, the porphyrin chromophores fold over the steroid skeleton so that straightforward analysis of the sign of the couplet cannot be correlated with the absolute stereochemistry. However, such porphyrin−steroid interactions would be reflected in shifts of the steroid protons in the ^{1}H NMR spectrum, which is not the case.

(25) Calculation of rotational strengths R_1 and R_2 from the experimental CD spectrum of **6b** in Figure 1 lead to an almost conservative coupling. However, in all measured CD spectra of porphyrin dimers the first Cotton effect has a higher $\Delta\epsilon$ value than the second which also bears a shoulder around 395 nm.

Scheme 2

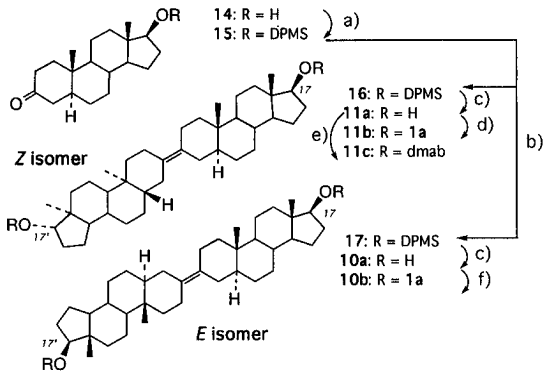

a) DPMSCl, imidazole, CH_2Cl_2, rt, 12 h, 89%; b) $TiCl_3$, $LiAlH_4$, THF, reflux, 20 h, 24% (**16** and **17**); c) TBAF, THF, rt, 3 h, 92% (**10a** and **11a**); d) 1, EDC, DMAP, CH_2Cl_2, rt, 12 h, 58%; e) *p*-dimethylaminobenzoyl triazol, DBU, CH_2Cl_2, rt,12 h, 45%; f) see d), 70%.

interchromophoric distances 22−24 Å, with the corresponding bis(dimethylaminobenzoates) **7c**, **9c**, and bisbenzoate **9d**, show the dramatic increase in sensitivity in the porphyrin series.[1]

29−34 Å Interchromophoric Distance. The dimeric steroids[26] **10a** and **11a** were synthesized from stanolone **14** in order to explore the extent of long distance exciton coupling with the porphyrin chromophores (Scheme 2). Silylation (**15**) followed by McMurry-coupling[27] afforded dimers **16** and **17**, which were deprotected to 1,18-glycols **10a** and **11a**. The *Z*-isomer **11a**, mp >300 °C, was separated from the *E*-isomer **10a** by crystallization from CH_2Cl_2. Both isomers were derivatized to the corresponding porphyrin dimers **10b** and **11b**; **11a** was also converted to the bis(*p*-dimethylaminobenzoate) **11c**.

CD spectra of **11b** ($A = +32$) and **10b** ($A = +11$) are shown in Figure 2. The spectrum of bis(*p*-dimethylaminobenzoate) **11c**, the chromophore of choice in many applications of exciton coupled CD,[2] shows no coupling due to the smaller extinction (ϵ 28 200 for the isolated chromophore). Energy calculation of *Z*-isomer **11b** with two parallel steroid backbones leads to a favorable projection angle between the 17-O/17′-O-bonds and an interchromophoric distance of ca. 34 Å; a positive couplet with $A = +32$ is the outcome. The bent geometry of the steroid moieties in **10b**, in contrast, results in the two chromophores being close to colinear, the outcome of which is a much smaller CD amplitude of +11. Although similarities in spectroscopic data of **10a**/**11a** and other similar dimeric steroids, i.e., synthetic cephalostatin analogs,[26c] preclude simple structural differentiation, the long distance coupling between the porphyrins can readily distinguish dimers **10b**/**11b**.

Compared to the CD spectra of steroids, the CD couplet for the *Z*-isomer **11b** is clearly nonconservative (first $\Delta\epsilon$ > second $\Delta\epsilon$), while the *E*-isomer **10b** exhibits only the positive band of the corresponding couplet; in both cases, the first CD Cotton effect is red-shifted with respect to the UV maximum (418 nm) (Figure 2). We found that independent of the spatial arrangement of the chromophores, such strong nonconservativity was not observed in the CD spectra of various 3,17-bisporphyrin steroid derivatives **7b**, **8b**, and **9b** (Table 1).

The question thus arises whether the Cotton effects observed in **10b** and **11b,** and in the brevetoxin bridged porphyrin dimers

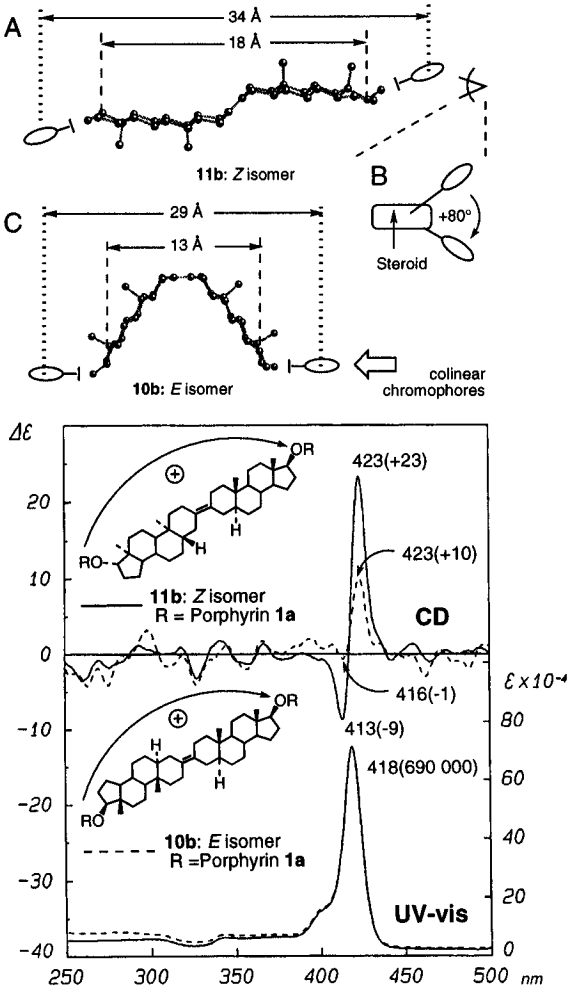

Figure 2. Above: Steroid backbone of *Z*-isomer **11b** (A) including side-view (B) and *E*-isomer **10b** (C), calcd by MacroModel 4.5.[37] Ellipsoids denote porphyrins. Distances between the chiral centers and the centers of chromophores are indicated. Below: CD- and UV/vis data of **11b** (solid, $c = 0.9$ μM) and **10b** (dashed, $c = 0.9$ μM).

(see below) are long-distance exciton couplings or not. Jacques and co-workers explained the nonconservative CD couplets in 2α(or β),17β-A-nor-5α-androstanes dimethoxybenzoates by nonexciton coupled Cotton effects overlapping on the weak exciton couplet.[8] Since the CD spectra of steroid monoporphyrin derivatives exhibited only negligible Cotton effects under the dilute concentrations we employed for measuring the bisporphyrin derivatives, it is clear that the chiral perturbation of the porphyrin chromophore by the steroidal nucleus is negligible.

The reason for the reduced intensity of the second Cotton effect and especially in the bisporphyrin derivatives with large interchromophoric distances is still not understood. If the Soret components were only interacting among themselves, the two components of the exciton couplet should have rotational strengths of equal magnitude. The observed imbalance indicates that the Soret transitions are coupling with other transitions to a significant extent. All measured CD spectra, e.g., those of **6b** (Figure 1C), do not show detectable intensity in the visible region or in the ultraviolet down to 250 nm. This excludes coupling of the Soret band with the Q, N, and L bands of the porphyrins.[20,21] The absence of significant Soret rotational strength in the monoporphyrin derivatives excludes the possibility of Soret coupling with high-energy transitions in the steroid skeleton. Coupling of the Soret transitions in one porphyrin with the high-energy transitions in the other porphyrin has not been excluded experimentally and is being investigated

(26) Dimeric steroids have attracted attention because of the high antitumor activity of cephalostatins isolated from marine animals *Cephalodiscus*: (a) Pettit, G. R.; Inoue, M.; Kamano, Y.; Herald, D. L.; Arm, C.; Dufresne, C.; Christie, D. N.; Schmidt, J. M.; Doubek, D. L.; Krupa, T. S. *J. Am. Chem. Soc.* **1988**, *110*, 2006. (b) Jeong, J. U.; Fuchs, P. L. *J. Am. Chem. Soc*. **1994**, *116*, 773. (c) Heathcock, C. H.; Smith, S. C. *J. Org. Chem.* **1994**, *59*, 6828.

(27) McMurry, J. E. *Chem. Rev.* **1989**, *89*, 1513.

Chart 1

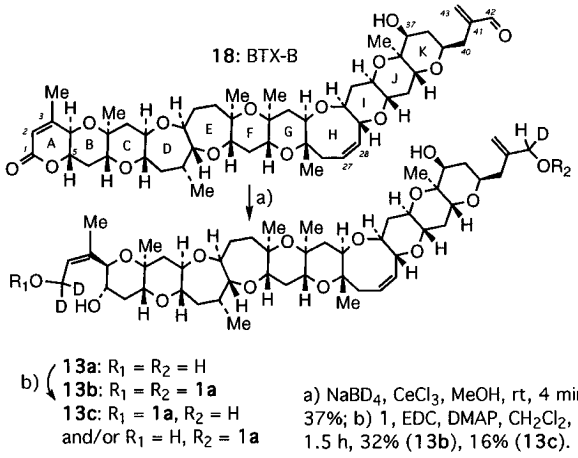

theoretically. For practical and theoretical reasons, it would be interesting to see whether the trends observed in these nonconservative coupling arising from the weak porphyrin/porphyrin interaction over a long distance is a general feature or not.[28]

Up to 50 Å Interchromophoric Distance. The interchromophoric distance is ca. 50 Å in the brevetoxin B (BTX-B)-bridged porphyrin dimer **13b**, which was prepared by selective reduction[29] of BTX-B **18** (red-tide toxin) followed by selective esterification (Chart 1). The absolute configuration of BTX-B was determined by exciton coupled CD of the bis-*p*-bromobenzoate of the vicinal 27,28-diol (obtained by oxidation of 27-ene),[30] by X-ray[31] and more recently by total synthesis.[32] Molecular modeling of **18** showed that the cigar-shaped skeleton can be bent at two flexible moieties in the backbone, the eight-membered ring H and the two seven-membered rings D and E.[33] These flexible moieties in the middle of the rigid *trans*-fused backbones are a common feature of brevetoxins and ciguatoxins and are suspected to play key roles in the bioactivities of these toxins;[34,35] however, as yet no conformational studies in solution have been performed.

In nonpolar solvents such as CH_2Cl_2 or toluene, the CD of bisporphyrin ester **13b** is devoid of Cotton effects. However, a bisignate CD is observed in the more polar and protic solvent MeOH/water 4/1, $A = -7.0$ (Figure 3). The fact that the porphyrin monoester **13c** exhibited no CD under the same conditions shows that the chiral centers are too remote from the chromophores; more importantly, it also demonstrates that the bisignate CD observed in bis ester **13b** is not due to stacking. Thus the couplet observed for the porphyrin dimer **13b** must be caused by exciton coupling over a distance of up to 50 Å between the porphyrin chromophores. The appearance of exciton coupling in MeOH/water 4/1 shows that this solvent system leads to conformational changes which favor coupling between the porphyrin electric transition moments. The amplitude is increased to −10.5 by saturating the solution with CsCl (Figure 3); this increase is possibly caused by complexation of the large, polarizable Cs^+ to multiple oxygens in the toxin backbone, resulting in a shift from a cigar to a bent shaped conformer of the skeleton.[36]

Short Interchromophoric Distance. Due to the short interchromophoric distance and favorable dihedral angle, a most intense couplet would have been expected for the 1*R*,2*R*-cyclohexanediol bridged porphyrin dimer **12b** (Figure 4). Surprisingly, however, the amplitude $A = -400$ is significantly smaller than that of 1,4-bisester **6b** ($A = +675$) (Table 1). Split porphyrin signals in the ^{1}H NMR spectrum of **12b**, measured at 25 °C in DMSO-d_6, suggested the presence of a mixture of cyclohexane conformers in which the porphyrin protons are differently exposed to the ring current effects of the two porphyrin cores (Figure 4a). This assumption was confirmed by the enhanced signal resolution in the spectrum measured at 100 °C due to fast equilibrium between cyclohexane conformers (Figure 4b). According to calculations by MacroModel,[37] the most stable conformer is **12c** with axial bulky substituents; this is followed by boat conformers **12d**, **12e**, then **12f**, and finally the normal chair form **12g** (+34 kJ/mol) with two eq *s-trans* esters. The twist of the effective transition moments (Figure 1B) give rise to a negative couplet in **12d**, **12e**, **12g**, a positive couplet in **12f**, and no Cotton effect in **12c**. Conformational changes of the cyclohexane ring were also reflected in the difficulties encountered in derivatising 1,2-glycol **12a**. Thus, for compounds with vicinal chiral centers, porphyrins should be used with caution because of possible conformational anomalies.[38]

Conclusions

General distance screening of the exciton coupled CD by porphyrin reporter groups exemplified by **1** show substantial coupling even at a distance of ca. 50 Å. In all cases exciton

(28) In weakly coupled chromophores, i.e., those with interchromophoric dipole−dipole coupling energy weaker than the half band width of the monomer absorption, one of us (R.W.) has demonstrated that calculations using polarizability theory instead of exciton theory may provide additional insight in the shape of bisignate curves.[13] These calculations further predicted the possibility of porphyrin/porphyrin interactions covering a distance of 40 Å or more. Since the analysis of CD spectra of multiheme proteins is not straightforward due to the dominating effects from the protein environment, the long distance porphyrin/porphyrin interactions observed with the dimeric steroid and brevetoxin bridges favor the possibility of heme/heme long distance interactions in multiheme proteins as well. A theoretical analysis of the results presented here will be published elsewhere.

(29) Qin, G.-W.; Nakanishi, K. Unpublished results.

(30) (a) Lin, Y.-Y.; Risk, M.; Ray, S. M.; Van Engen, D; Clardy, J.; Golik, J.; James, J. C.; Nakanishi, K. *J. Am. Chem. Soc.* **1981**, *103*, 6773. (b) Lee, M. S.; Repeta, D. J.; Nakanishi, K.; Zagorski, M. G. *J. Am. Chem. Soc.* **1986**, *108*, 7855.

(31) Shimizu, Y.; Bando, H.; Chou, H.-N.; Van Dyne, G.; Clardy, J. C. *J. Chem. Soc., Chem. Commun.* **1986**, 1656.

(32) (a) Nicolaou, K. C.; Theodorakis, E. A.; Rutjes, F. P. J. T.; Tiebes, J.; Sato, M.; Untersteller, E.; Xiao, X.-Y. *J. Am. Chem. Soc.* **1995**, *117*, 1171. (b) Nicolaou, K. C.; Rutjes, F. P. J. T.: Theodorakis, E. A.; Tiebes, J.; Sato, M.; Untersteller, E. *J. Am. Chem. Soc.* **1995**, *117*, 1173.

(33) (a) Rein, K. S.; Baden, D. G.; Gawley, R. E. *J. Org. Chem.* **1994**, *59*, 2101. (b) Rein, K. S.; Lynn, B.; Gawley, R. E.; Baden, D. G. *J. Org. Chem.* **1994**, *59*, 2107.

(34) Yasumoto, T.; Murata, M. *Chem. Rev.* **1993**, *93*, 1897.

(35) Brevetoxin B is a voltage sensitive sodium channel opener.[33] However, we have shown that brevetoxin B itself is capable of forming cation specific "channels" in lipid bilayers: Matile, S.; Nakanishi, K. *Angew. Chem.* **1996**, *108*, 812. The mono- and bisporphyrin derivatives **13b** and **13c** were employed in investigating the nature and properties of these "channels" formed by brevetoxin B as well as differentiating between CD couplets caused by "channel" formation and stacking: Matile, S.; Berova, N.; Nakanishi, K. Submitted for publication.

(36) Addition of TBA chloride to the MeOH/water 4:1 solution of **13b** *decreases* the CD amplitude. The effect of Cs^+ is therefore likely to be caused by complexation of the metallic ion rather than increase in medium polarity.

(37) Mohamadi, F.; Richards, N. G. J.; Guida, W. C.; Liskamp, R.; Caufield, C.; Chang, G.; Hendrickson, T.; Still, W. C. *J. Comput. Chem.* **1990**, *11*, 440.

(38) During the preparation of this manuscript, an 1*S*,2*S*-cyclohexanediamine-bridged porphyrin dimer was described (Ema, T.; Nemugaki, S.; Tsuboi, S.; Utaka, M. *Tetrahedron Lett.* **1995**, *36*, 5905). The opposite sense of the observed couplet is to be expected from the opposite absolute configurations. The significantly smaller amplitude is in part due to a smaller oscillator strength for *mono*-phenylporphyrin used by Ema *et al.* as compared with the *tetra*-phenylporphyrin used here. Correcting for this effect, based upon the dipole strength reported for a 5-(1′-naphthyl)porphyrin,[14a] the magnitude of couplet observed by Ema et al. would be increased from 113 to 248, much closer to the magnitude of 400 observed in this work for **12b**. The remaining discrepancy can probably be attributed to differences in conformational averaging for the bisamide *vs* the bisester. Ema *et al.* do not discuss the possibility of multiple conformers.

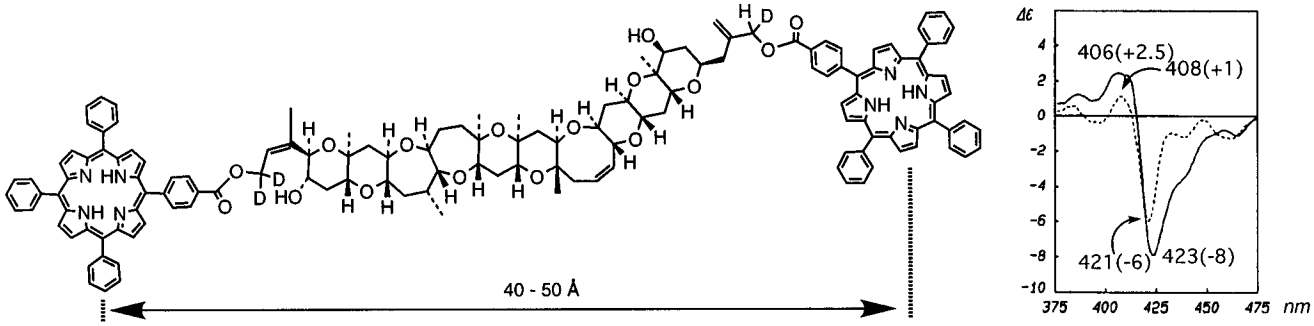

Figure 3. Structure and CD spectra of brevetoxin-bridged porphyrin dimer **13b** in MeOH/water 4/1 in the presence (solid) and absence (dotted) of CsCl, $c = 1.0$ μM.

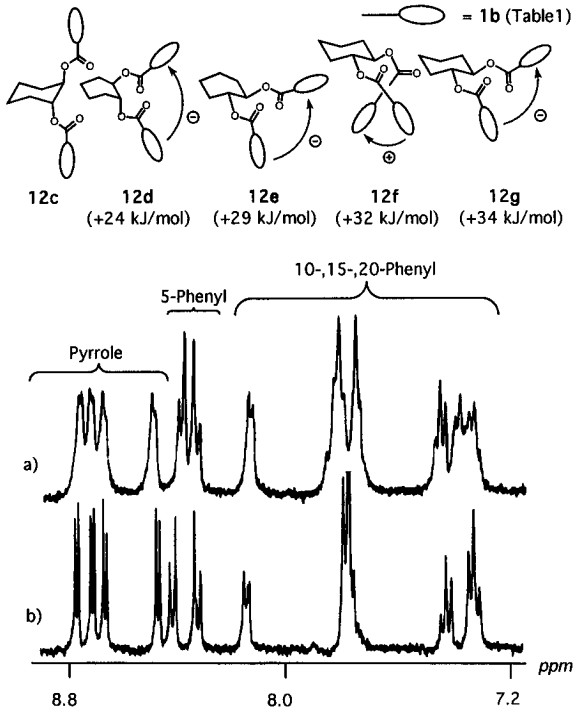

Figure 4. The five most stable conformers of the bisporphyrin **12b**, calcd by MacroModel4.5;[37] 400 MHz ^{1}H NMR of **12b**, in DMSO-d_6 at (a) 25 °C and (b) 100 °C.

coupled CD of bisporphyrin esters correctly represent the chiral sense of twist between the C−O bonds at the corresponding stereogenic centers, thus leading to the conclusion that for interpreting exciton coupled CD curves, the effective transition moment can be regarded as being in the 5,15-direction of the porphyrin skeleton as shown in Figure 1B.

Application of porphyrins to compounds with vicinal chiral centers is restricted by possible conformational changes; on the other hand, steric interactions (repulsion or stacking) of the bulky chromophores may be useful to stabilize distinct conformers in flexible (acyclic) compounds[39] or to investigate higher energy conformers such as **12c**. Porphyrin chromophores attached to dimeric steroids revealed that application of exciton coupled CD to microscale assignment of absolute configurations can be extended to compounds with a distance of 18 Å between stereogenic centers. Furthermore, porphyrins attached to brevetoxin B revealed that the conformational studies by exciton coupled CD can be extended further to compounds with a distance of at least 35 Å between the stereogenic centers. Thus the porphyrin chromophores have extended the interchromophoric coupling distance from ca. 15 Å bis(dimethylaminobenzoate) to at least 50 Å. They constitute the most powerful chromophores available for the exciton coupled CD method so far. Conformational studies of various porphyrin derivatives of BTX and application of porphyrin reporter groups to structural studies of biopolymers such as membranes, proteins, nucleic acids, etc., are ongoing.[40]

(39) The attachment of **1** to *acyclic* chiral diol/diamines leads to stereocontrolled porphyrin π,π-stacking, and the resulting CD spectra allows the straightforward determination of the absolute configuration of single chiral centers: Matile, S.; Berova, N.; Nakanishi, K. *Enantiomer*, in press. Scope and limitations of this new concept are under ongoing investigation.

Experimental Section

General Procedures. Solvents employed were reagent grade. Anhydrous solvents were dried and distilled (THF from Na/benzophenone, CH_2Cl_2 from CaH_2). Acetonitrile was dried over molecular sieves (4 Å). Unless otherwise noted, materials were obtained from commercial suppliers and were used without further purification. All reactions were performed in dried glassware under argon. Reactions were followed by thin-layer chromatography (TLC) using Whatman alumina sheets, coated with silica gel (4 × 10 cm, 250 μm, UV_{254}), and reported as retention factors (R_f). Microscale preparative TLC (PTLC) was performed using Whatman thin layer chromatography plates (K5F, 20 × 20 cm, silica gel 150 Å, 250 μm, UV_{254}). Column chromatography (CC) was performed using ICN silica gel (32−63 mesh). HPLC purifications were performed using a Waters HPLC system equipped with a Waters 600 E Multisolvent Delivery System, a Waters 600 Controller and a Waters 996 Photodiode Array Detector using the Millenium 2010 software for data processing. Melting points were measured on a Thomas Hoover Capillary Melting Point Apparatus (uncorrected). UV−vis spectra were recorded as CH_2Cl_2 solutions on a Perkin-Elmer Lambda 4B spectrophotometer and reported as λ_{max} [nm] (ϵ_{max} [L mol^{-1} cm^{-1}]). IR spectra were obtained as CCl_4 solutions using a NaCl microcell on a Perkin Elmer 1600 FT-IR spectrophotometer. ^{1}H-NMR spectra and ^{13}C-NMR spectra were obtained on a Varian VXR400 or Varian VXR300 and are reported in parts per million (ppm) relative to TMS (δ), with coupling constants (J) in hertz (Hz). Low-resolution and high-resolution FAB mass spectra were measured on a JEOL JMS-DX303 HF mass spectrometer using a glycerol matrix and Xe ionizing gas. CI mass spectra were measured on a NERMAG R10-10 spectrometer with NH_3 as ionizing gas. CD spectra were recorded as CH_2Cl_2 solutions on a JASCO J-720 spectropolarimeter driven by a JASCO DP700N data processor, respectively, and reported as λ_{max} [nm] ($\Delta\epsilon_{max}$ [L mol^{-1} cm^{-1}]). Smoothing and other manipula-

(40) One major concern which applies to every labeling technique is the question of the extent to which the introduced labels disturb a conformationally flexible system. As it has already been demonstrated in the case of philanthotoxins, the enormous amount of information available about interactions of porphyrins with themselves, proteins, nucleic acids, and membranes could be very useful in order to avoid or reduce such undesired effects (Huang, D.; Matile, S.; Berova, N.; Nakanishi, K. *Heterocycles* **1996**, *42*, 732). However, while oligonucleotides forming straight duplexes for example appear to be very attractive for studies of polymorphism and drug binding by exciton coupled CD between appropriately selected porphyrin chromophores, more precautions are necessary in case of kinked and flexible duplexes (Mahtab, R.; Rogers, J. P.; Murphy, C. J. *J. Am. Chem. Soc.* **1995**, *117*, 9099). Extensive model studies with porphyrin-labeled polypeptides and oligonucleotides thus will be required to delineate the scope and limitations of the porphyrin-reported exciton coupled CD method applied to biopolymers.

tions of spectra were carried out with a software developed in house: DFT (discrete Fourier transform) procedure.

5-(4′-Carboxymethylphenyl)-10,15,20-triphenylporphin (5). To a mixture of 4-carboxymethylbenzaldehyde (**2**, 4.104 g, 25 mmol), benzaldehyde (**3**, 7.960 g, 75 mmol), and $Zn(OAc)_2$ (5.480 g, 25 mmol) in propionic acid (500 mL) was added pyrrole (**4**, 6.710 g, 100 mmol) at 100 °C within 1 h under vigorous stirring. The resulting dark solution was refluxed for further 4 h and then cooled to room temperature. The solvent was evaporated (15 Torr, 80 °C), and the solid residue was subjected to CC (SiO_2, 40 g, 7 × 45 cm, CH_2Cl_2). All product containing fractions were collected. The volume was reduced to 100 mL (15 Torr), and pyridine (2 mL) and an excess of DDQ (2 g) were added at room temperature. The resulting mixture was refluxed until the oxidation was complete (1 h), monitored by the disappearance of the absorption at 626 nm. Cooled to room temperature, the solution was extracted with 18% aqueous HCl solution (3 × 100 mL), neutralized with saturated aqueous $NaHCO_3$ solution (3 × 100 mL), washed with brine (1 × 100 mL), dried (Na_2SO_4), and evaporated (15 Torr) to give 11.5 g of black-purple crude product. Purification by CC (SiO_2, 30 g, 3.5 × 30 cm, CH_2Cl_2) yielded pure **5** (1.23 g, 7.5%) as deep purple crystals. TLC (CH_2Cl_2) R_f 0.74; mp >300 °C; UV−vis (MeCN) 645 (4600), 588 (4500), 545 (7000), 511 (15 900), 413 (353 000), 365 (sh, 33 000); UV−vis (CH_2Cl_2) 645 (4400), 589 (4450), 549 (6900), 514 (15 700), 418 (371 000), 365 (sh, 31 500); IR (CCl_4) 1718, 1285; ^{1}H NMR (400 MHz, $CDCl_3$) δ −2.64 (s, 2 H, exchange with D_2O), 4.13 (s, 3 H), 7.75−7.80 (m, 9 H), 8.22−8.25 (m, 6 H), 8.32 (d, 2 H, J = 8.14 Hz), 8.46 (d, 2 H, J = 8.14 Hz), 8.85−8.89 (m, 8 H); FAB-MS *m/z* 673 (M + H$^+$); FAB-HRMS *m/z* for $C_{46}H_{33}N_4O_2$, calcd 673.2603, found 673.2598; CD (MeOH) -; CD (CH_2Cl_2) -.

5-(4′-Carboxyphenyl)-10,15,20-triphenylporphin (TPP, 1). To a solution of **5** (1.10 g, 1.63 mmol) in EtOH (50 mL) was added 2 N NaOH (100 mL), and the suspension was refluxed for 4 h. Cooled to room temperature, the solvent was decanted, and the crude product was washed with water (2 × 50 mL), MeOH (3 × 20 mL), and hexane (2 × 50 mL). Evaporation (15 Torr and 0.01 Torr) gave anal. pure **1** (922 mg, 86%) as a deep purple powder. Mp >300 °C; UV−vis (MeOH) 645 (4600), 588 (4500), 545 (7000), 511 (15 900), 413 (353 000), 365 (sh, 33 000); IR (CCl_4) 3444, 1639, 1211; ^{1}H NMR (400 MHz, $CDCl_3$/CD_3OD 4:1) δ −3.00 to −2.00 (br s, ca. 2 H), 7.74−7.80 (m, 9 H), 8.21−8.24 (m, 6 H), 8.35 (d, 2 H, J = 8.05 Hz), 8.51 (d, 2 H, J = 8.05 Hz), 8.81−8.83 (m, 8 H); FAB-MS *m/z* 659 (M + H$^+$); FAB-HRMS *m/z* for $C_{45}H_{31}N_4O_2$, calcd 659.2446, found 659.2457.

5α-Cholestane-3β,6α-diol Bis(*p*-[10′,15′,20′-triphenyl-5′-porphyrinyl]benzoate) (6b). To a solution of **1** (24.4 mg, 37.1 μmol), EDC (7.1 mg, 37.1 μmol), and DMAP (4.0 mg, 37.1 μmol) in absolute CH_2Cl_2 (1 mL) was added (room temperature) a solution of **6a** (5 mg, 12.4 μmol) in CH_2Cl_2 (1 mL). The mixture was stirred (room temperature, 12 h), diluted with CH_2Cl_2 (20 mL), extracted with a solution of saturated aqueous NH_4Cl (3 × 20 mL), washed with brine (2 × 20 mL), dried (Na_2SO_4), and evaporated (15 Torr) to give 29 mg (139%) of crude product, which was purified by CC (SiO_2, 2 × 25 cm, 20 g, CH_2Cl_2/hexane 3:1, R_f 0.36) to yield pure **6b** (16.3 mg, 78%) as a deep purple powder. TLC (CH_2Cl_2/hexane 3:1) R_f 0.36; mp >300 °C; UV−vis (CH_2Cl_2) 645 (8200), 589 (8300), 549 (12 800), 514 (29 200), 418 (690 000); IR (CCl_4) 2949, 2880, 1713, 1547, 1252, 1218, 1110, 1068, 1000, 978; ^{1}H NMR (400 MHz, $CDCl_3$) δ −2.64 (s, 2 H, exchange with D_2O), 0.74−2.55 (several m, 44 H), 5.23−5.34 (br m, 2 H), 7.67−7.83 (2m, 18 H), 8.21−8.29 (m, 12 H), 8.31, 8.36 (2d, 4 H, J = 8.06 Hz), 8.48, 8.50 (2d, 4 H, J = 8.06 Hz), 8.85−8.89 (m, 16 H); FAB-MS *m/z* 1685 (M + H$^+$); FAB-HRMS *m/z* for $C_{117}H_{105}N_8O_4$ calcd 1685.8280, found 1685.8260.

5α-Androstane-3α,17β-diol Bis(*p*-[10′,15′,20′-triphenyl-5′-porphyrinyl]benzoate) (7b). Following the procedure for **6b**, **7a** (7.6 mg, 11.5 μmol) was converted to 12.0 mg (135%) of crude product, which was purified by CC (SiO_2, 2 × 25 cm, 20 g, CH_2Cl_2, R_f 0.69) to yield pure **7b** (6.5 mg, 73%) as a deep purple powder. TLC (CH_2Cl_2) R_f 0.69; mp >300 °C; UV−vis (CH_2Cl_2) 645 (8200), 589 (8300), 549 (12 800), 514 (29 200), 418 (690 000); IR (CCl_4) 2940, 2875, 1710, 1547, 1252, 1218, 1110, 1068, 1000, 978; ^{1}H NMR (400 MHz, $CDCl_3$) δ −2.64 (s, 2 H, exchange with D_2O), 0.93−2.50 (several m, 22 H), 0.99, 1.12 (2s, 2 CH_3), 5.02 (t, 1 H, J = 8.42 Hz), 5.49−5.52 (m, 1 H), 7.74−7.79 (m, 18 H), 8.21−8.25 (m, 12 H), 8.29, 8.36 (2d, 4 H, J = 8.06 Hz), 8.42, 8.49 (2d, 4 H, J = 8.06 Hz), 8.78−8.90 (m, 16 H); FAB-MS *m/z* 1473 (M + H$^+$); FAB-HRMS *m/z* for $C_{109}H_{89}N_8O_4$ calcd 1573.7010, found 1573.7030.

5α-Androstane-3α,17β-diol Bis(*p*-dimethylaminobenzoate) (7c). A solution of **7a** (4.0 mg, 13.6 μmol), *p*-dimethylaminobenzoyl triazol[4c] (20 mg, 92.6 μmol), and DBU (5.4 mg, 35.4 μmol) in absolute CH_2Cl_2 (1 mL) was stirred at room temperature for 24 h, diluted with CH_2Cl_2 (20 mL), extracted with a solution of saturated aqueous NH_4Cl (3 × 20 mL), washed with brine (2 × 20 mL), dried (Na_2SO_4), and evaporated (15 Torr) to give 10.0 mg (132%) of crude product, which was purified by PTLC (SiO_2, CH_2Cl_2, R_f 0.10, 2×) to yield pure **7c** (5.3 mg, 75%) as a slightly yellow powder. TLC (CH_2Cl_2/MeOH 20:1) R_f 0.33; mp 218−220 °C; UV−vis (CH_2Cl_2) 310 (53 200); IR (CCl_4) 2932, 2863, 1705, 1547, 1252, 1217, 1107, 1068, 1004, 978; ^{1}H NMR (400 MHz, $CDCl_3$) δ 0.80−2.30 (several m, 22 H), 0.86, 0.93 (2s, 2 CH_3), 3.04, 3.05 (2s, $N(CH_3)_2$), 4.80 (t, 1 H, J = 9.07 Hz, H-C(17)), 5.22−5.24 (m, 1 H), 6.65, 6.67 (2d, 4 H, J = 5.41 Hz), 7.91, 7.93 (2d, 4 H, J = 5.41 Hz); FAB-MS *m/z* 586 (100, M$^+$); FAB-HRMS *m/z* for $C_{37}H_{50}N_2O_4$ calcd 586.3771, found 586.3775.

5α-Androstane-3β,17α-diol Bis(*p*-[10′,15′,20′-triphenyl-5′-porphyrinyl]benzoate) (8b). Following the procedure for **6b**, **8a** (3.6 mg, 12.33 μmol) was converted to 19.0 mg (130%) of crude product, which was purified by CC (SiO_2, 2 × 25 cm, 20 g, CH_2Cl_2, R_f 0.66) to yield pure **8b** (11.1 mg, 75%) as a deep purple powder. TLC (CH_2Cl_2) R_f 0.69; UV−vis (CH_2Cl_2) 645 (8200), 589 (8300), 549 (12 800), 514 (29 200), 418 (690 000); ^{1}H-NMR (400 MHz, $CDCl_3$) δ −2.67 (s, 2 H, exchange with D_2O), 0.93−2.50 (several m, 22 H), 0.96, 1.02 (2s, 2 CH_3), 5.09−5.16 (m, 1 H), 5.27 (d, 1 H, J = 6.23 Hz), 7.74−7.81 (m, 18 H), 8.21−8.26 (m, 12 H), 8.29, 8.36 (2d, 4 H, J = 8.04 Hz), 8.43, 8.49 (2d, 4 H, J = 8.06 Hz), 8.79−9.00 (m, 16 H).

5α-Androstane-3β,17β-diol Bis(*p*-[10′,15′,20′-triphenyl-5′-porphyrinyl]benzoate) (9b). Following the procedure for **6b**, **9a** (1.1 mg, 7.6 μmol) was converted to 7.0 mg (118%) of crude product, which was purified by PTLC (SiO_2, CH_2Cl_2, R_f 0.35) to yield pure **9b** (3.8 mg, 64%) as a deep purple powder. TLC (CH_2Cl_2) R_f 0.35; UV−vis (CH_2Cl_2) 645 (8200), 589 (8300), 549 (12 800), 514 (29 200), 418 (690 000); ^{1}H NMR (400 MHz, $CDCl_3$) δ −2.63 (s, 2 H, exchange with D_2O), 0.93−2.50 (several m, 22 H), 0.97, 1.05 (2s, 2 CH_3), 5.02 (t, 1 H, J = 8.42 Hz), 5.11−5.19 (m, 1 H), 7.73−7.85 (m, 18 H), 8.16−8.22 (m, 12 H), 8.34, 8.36 (2d, 4 H, J = 8.04 Hz), 8.44 (d, 8 H, J = 8.06 Hz), 8.80−9.00 (m, 16 H).

5α-Androstane-3β,17β-diol Bis(*p*-dimethylaminobenzoate) (9c). Following the procedure for **7c**, **9a** (4.0 mg, 13.6 μmol) was converted to 7.5 mg (100%) of crude product, which was purified by PTLC (SiO_2, CH_2Cl_2/MeOH 40:1 R_f 0.62) to yield pure **9c** (5.8 mg, 77%) as a slightly yellow powder. TLC (CH_2Cl_2/MeOH 40:1) R_f 0.62; mp 221−224 °C; UV−vis (CH_2Cl_2) 310 (53 200); ^{1}H NMR (400 MHz, $CDCl_3$) δ 0.80−2.30 (several m, 22 H), 0.90, 0.93 (2s, 2 CH_3), 3.05 (s, 2 $N(CH_3)_2$), 4.80 (t, 1 H, J = 9.07 Hz), 4.85−4.94 (m, 1 H), 6.65, 6.67 (2d, 4 H, J = 5.41 Hz), 7.90, 7.93 (2d, 4 H, J = 5.41 Hz).

1(*R*),2(*R*)-*trans*-Cyclohexanediol Bis(*p*-[10′,15′,20′-triphenyl-5′-porphyrinyl]benzoate) (12b). To a solution of **1** (15 mg, 22.8 μmol), EDC (7.1 mg, 37.1 μmol), and DMAP (4.0 mg, 37.1 μmol) in absolute CH_2Cl_2 (2 mL), a solution of **12a** (1.3 mg, 11.3 μmol) in CH_2Cl_2 (1 mL) was added (room temperature). The mixture was refluxed (4 h), diluted with CH_2Cl_2 (20 mL), extracted with a solution of saturated aqueous NH_4Cl (3 × 20 mL), washed with brine (2 × 20 mL), dried (Na_2SO_4), and evaporated (15 Torr) to give 15 mg (95%) of crude product, which was purified by CC (SiO_2, 2 × 25 cm, 20 g, CH_2Cl_2, R_f 0.56) to yield pure **12b** (8.5 mg, 54%) as a deep purple powder. TLC (CH_2Cl_2) R_f 0.56; mp >300 °C; UV−vis (MeCN) 644 (7100), 593 (8000), 551 (20 600), 513 (26 700), 419 (690 500); IR (CCl_4) 2918, 2857, 1717, 1598, 1550, 1348, 1269, 1251, 1110, 1097, 1001, 961; ^{1}H-NMR (400 MHz, $CDCl_3$) δ −2.70 (s, 2 H, exchange with D_2O), 1.2−2.5 (several m, 8 H), 5.57−5.63 (br m, 2 H), 7.50−7.62, 7.69−7.80 (2m, 18 H), 8.07−8.12, 8.18−8.22 (2m, 12 H), 8.29−8.54 (several d-lk m, 8 H), 8.68−8.99 (several m, 16 H); FAB-MS *m/z* 1397 (M + H$^+$); FAB-HRMS *m/z* for $C_{96}H_{69}N_8O_4$ calcd 1397.5440, found 1397.5447.

5α-Androstane-17β-diphenylmethylsilyloxy-3-one (15). A solution of stanolone **14** (480 mg, 1.655 mmol), DPMSCl (385 mg, 1.67 mmol), and imidazole (113 mg, 1.67 mmol) in absolute CH_2Cl_2 (50 mL) was stirred at room temperature for 15 h, diluted with CH_2Cl_2 (50

mL), extracted with a solution of saturated aqueous NH_4Cl (3 × 100 mL), washed with brine (1 × 100 mL), dried (Na_2SO_4), and evaporated (15 Torr) to give 906 mg (100%) of crude product, which was purified by CC (SiO_2, CH_2Cl_2, R_f 0.31) to yield pure **15** (716 mg, 89%) as a colorless oil. TLC (CH_2Cl_2) R_f 0.31; ^{1}H NMR (400 MHz, $CDCl_3$) δ 0.01 (s, $SiCH_3$) 0.60−2.33 (several m, 22 H), 0.62, 0.85 (2s, 2 CH_3), 3.67 (t, 1 H, J = 8.34 Hz), 7.34−7.42, 7.58−7.61 (2m, 10 H).

***Z*-Bis-5α-androstane-17*β*,17*β*′-diphenylmethylsilyloxy-3,3′-ene (16) and *E*-Bis-5α-androstane-17*β*,17*β*′-diphenylmethylsilyloxy-3,3′-ene (17).** To freshly distilled THF (15 mL), carefully degassed with Ar, $TiCl_3$ (3.39 g, 20.0 mmol) was added under Ar at room temperature. To the resulting violet suspension $LiAlH_4$ (362 mg, 9.53 mmol) was added at room temperature under Ar, and the mixture was refluxed for 15 min. Then a solution of **15** (137 mg, 0.28 mmol) in dry and degassed THF was added to the refluxing black suspension. Refluxing was continued until the intermediate diol (TLC (CH_2Cl_2/MeOH 40:1) R_f 0.68) was completely converted (20 h). Cooled to room temperature, the mixture was carefully poored into ice water (100 mL). Hexane (100 mL) was added, and the organic layer was extracted with water (4 × 100 mL), evaporated (15 Torr), dissolved in CH_2Cl_2 (100 mL), washed with brine (2 × 100 mL), dried (Na_2SO_4), and evaporated (15 Torr) to give 150 mg (109%) of crude product. Purification by CC (SiO_2, CH_2Cl_2/hexane 1:4 R_f 0.42) afforded a 1:1 mixture of the pure isomers **16/17** (30.9 mg, 24%) as a colorless solid. TLC (CH_2Cl_2/hexane 1:4) R_f 0.31; ^{1}H NMR (400 MHz, $CDCl_3$) δ 0.01 (s, 2 $SiCH_3$) 0.60−1.89 (several m, 40 H), 0.60, 0.82 (2s, 4 CH_3), 2.24−2.31, 2.52−2.62 (2 br d-lk m, 4 H), 3.65 (t, 2 H, J = 8.32 Hz), 7.34−7.42, 7.58−7.61 (2m, 20 H); CI-MS *m/z* 858 ($M + NH_4^+$).

***Z*-Bis-5α-androstane-3,3′-ene-17*β*,17*β*′-diol (11a) and *E*-Bis-5α-androstane-3,3′-ene-17*β*,17*β*′-diol (10a).** A 1:1 mixture of the isomers **16/17** (31 mg, 33 μmol) was solved in a 1 M solution of TBAF in THF (1 mL) and stirred at room temperature for 3 h. To the resulting mixture were added brine (50 mL) and hexane (50 mL) . The water layer was extracted with hexane (2 × 50 mL) and EtOAC (3 × 50 mL). The resulting EtOAc solution was reduced (50 mL), washed with brine (1 × 50 mL), dried (Na_2SO_4), and evaporated (15 Torr) to give 906 mg (100%) of crude product. The two isomers were separated by CC (SiO_2, CH_2Cl_2, R_f 0.52 (**11a**), R_f 0.48 (**10a**)). Crystallization of **11a** from CH_2Cl_2 afforded **11a** (6.9 mg, 32%) as a white powder, **10a** (7.5 mg, 42%) as a highly viscous oil, and an oily mixture of **10a/11a** (2.2 mg, 12%). **11a:** Because of the extremely low solubility of **11a** in all usual solvents, spectroscopic analysis is almost impossible. TLC (CH_2Cl_2) R_f 0.52; mp >300 °C; ^{1}H NMR (400 MHz, $CDCl_3$/CD_3OD 1:1) δ 0.6−2.4 (several m, 56 H), 3.61−3.64 (t-lk m, 2 H); FAB-, CI- or DCI-MS: no signal. **10a**: TLC (CH_2Cl_2) R_f 0.48; ^{1}H NMR (400 MHz, $CDCl_3$) δ 0.60−1.89 (several m, 40 H), 0.73, 0.86 (2s, 4 CH_3), 2.24−2.31, 2.52−2.62 (2 br d-lk m, 4 H), 3.61 (t, 2 H, J = 7.98 Hz); CI-MS *m/z* 548 (M^+).

***Z*-Bis-5α-androstane-3,3′-ene-17*β*,17*β*′-diol Bis(*p*-[10′,15′,20′-triphenyl-5′-porphyrinyl]benzoate) (11b).** Following the procedure for **6b**, **11a** (1.0 mg, 1.82 μmol) was converted to 3.3 mg (100%) of crude product, which was purified by PTLC (SiO_2, CH_2Cl_2/MeOH 40:1, R_f 0.65) to yield pure **11b** (2.3 mg, 70%) as a deep purple powder. TLC (CH_2Cl_2/MeOH 40:1) R_f 0.65; UV−vis (CH_2Cl_2) 645 (8200), 589 (8300), 549 (12 800), 514 (29 200), 418 (690 000); ^{1}H NMR (400 MHz, $CDCl_3$) δ −2.80 (s, 2 H, exchange with D_2O), 0.93−2.50 (several m, 44 H), 1.06, 1.10 (2s, 4 CH_3), 5.04 (t, 2 H, J = 7.69 Hz), 7.71−7.80 (m, 18 H), 8.11−8.27 (m, 12 H), 8.29 (d, 4 H, J = 8.30 Hz), 8.42 (d, 4 H, J = 8.30 Hz), 8.77−8.98 (m, 16 H); FAB-MS *m/z* 1828 (M^+).

***E*-Bis-5α-androstane-3,3′-ene-17*β*,17*β*′-diol Bis(*p*-[10′,15′,20′-triphenyl-5′-porphyrinyl]benzoate) (10b).** Following the procedure for **6b**, **10a** (1.0 mg, 1.82 μmol) was converted to 3.5 mg (106%) of crude product, which was purified by PTLC (SiO_2, CH_2Cl_2/MeOH 40:1, R_f 0.62) to yield pure **10b** (2.3 mg, 70%) as a deep purple powder. TLC (CH_2Cl_2/MeOH 40:1) R_f 0.62; UV−vis (CH_2Cl_2) 645 (8200), 589 (8300), 549 (12 800), 514 (29 200), 418 (690 000); ^{1}H NMR (400 MHz, $CDCl_3$) δ −2.80 (s, 2 H, exchange with D_2O), 0.93−2.50 (several m, 44 H), 1.06, 1.10 (2s, 4 CH_3), 5.04 (t, 2 H, J = 7.69 Hz), 7.71−7.80 (m, 18 H), 8.11−8.27 (m, 12 H), 8.29 (d, 4 H, J = 8.30 Hz), 8.42 (d, 4 H, J = 8.30 Hz), 8.77−8.98 (m, 16 H); FAB-MS *m/z* 1828 (M^+).

***Z*-Bis-5α-androstane-3,3′-ene-17*β*,17*β*′-diol Bis-(*p*-dimethylaminobenzoate) (11c).** Following the procedure for **7c**, **11a** (1.0 mg, 1.82 μmol) was converted to 1.5 mg (99%) of crude product, which was purified by PTLC (SiO_2, CH_2Cl_2/MeOH 40:1, R_f 0.36) to yield pure **11c** (0.7 mg, 45%) as a deep purple powder. TLC (CH_2Cl_2/MeOH 40:1) R_f 0.36; UV−vis (CH_2Cl_2) 310 (53 200); ^{1}H NMR (400 MHz, $CDCl_3$) δ 0.80−2.30 (several m, 40 H), 0.91, 0.94 (2s, 4 CH_3), 2.24−2.31, 2.55−2.64 (2 br d-lk m, 4 H), 3.05 (s, 2 $N(CH_3)_2$), 4.78 (t, 2 H, J = 8.97 Hz), 6.67 (d, 4 H, J = 5.40 Hz), 7.91 (d, 4 H, J = 5.40 Hz); FAB-MS *m/z* 843 ($M + H^+$); FAB-HRMS *m/z* for $C_{56}H_{78}N_2O_4$ calcd 842.5962, found 842.5947.

BTX-D(1,1,42)-1,42-diol (13a). BTX-B (**18**, 2.0 mg, 2.2 μmol) was dissolved in a solution of $CeCl_3$ (0.8 mg, 2.2 μmol) and $NaBD_4$ (0.4 mg, 10.0 μmol) in absolute MeOH (1 mL), stirred for 4 min at room temperature, filtered off through Celite, dried (Na_2SO_4), and evaporated (15 Torr) to give a crude product, which was purified by CC (CH_2Cl_2/MeOH 9:1, R_f 0.45) to yield pure **13a** (0.7 mg, 37%) as a colorless powder. (As a second main product, the selectively 42-reduced, 42-D-labeled BTX (0.8 mg, 42%) was isolated (CH_2Cl_2/MeOH 9:1, R_f 0.73) and characterized and will be used for further BTX-membrane studies.) TLC (CH_2Cl_2/MeOH 9:1) R_f 0.45; ^{1}H NMR (400 MHz, $CDCl_3$) δ 1.02, 1.04 (d, 3 H), 1.17 (s, 3 H), 1.24 (s, 3 H), 1.29 (s, 9 H), 1.47−1.90, 1.95−2.14, 2.14−2.28, 2.30−2.44 (4m, ca. 28 H), 2.65−2.67 (m, 1 H), 2.95−3.14, 3.18−3.44, 3.50−3.62 (3m, ca. 13 H), 3.79−3.81 (m, 1 H), 3.84−3.89 (dd-lk m, 1 H) 3.91−3.97 (dd-lk m, 2 H), 4.02−4.12 (m, 2 H), 4.37−4.39 (d-lk m, 1 H), 4.71−4.74 (m, 1 H), 4.91−4.95 (m, 1 H) 5.09−5.13 (m, 1 H), 5.76−5.80 (m, 2 H), 5.81−5.85 (m, 1 H); ^{2}H NMR (46 MHz, $CHCl_3$) 3.96−4.19; CI-MS *m/z* 922 ($M + NH_4^+$)

BTX-D(1,1,42)-1,42-diol Bis(*p*-[10′,15′,20′-triphenyl-5′-porphyrinyl]benzoate) (13b) and BTX-D(1,1,42)-1,42-ol *p*-(10′,15′,20′-triphenyl-5′-porphyrinyl)benzoate (13c). To a solution of **1** (3.0 mg, 4.6 μmol), EDC (0.9 mg, 4.6 μmol), and DMAP (0.5 mg, 4.6 μmol) in absolute CH_2Cl_2 (1 mL), a solution of **13a** (0.7 mg, 0.78 μmol) in CH_2Cl_2 (1 mL) was added (room temperature). The mixture was stirred (room temperature, 1.5 h), until almost all **13a** was consumed and four purple spots were visible on TLC (CH_2Cl_2/MeOH 40:1, R_f 0.36, R_f 0.28, R_f 0.17, R_f 0.14, ratio ca. 10:10:2:3). Then, the reaction mixture was diluted with CH_2Cl_2 (10 mL), extracted with a solution of saturated aqueous NH_4Cl (10 mL), washed with brine (10 mL), dried (Na_2SO_4), and evaporated (15 Torr) to give crude product, which was purified by PTLC (CH_2Cl_2/MeOH 40:1) to yield pure **13b** (0.5 mg, 32%) and **13c** (0.2 mg, 16%) as a deep purple powder. (As another main product, the 1,5,42-porphyrin trimer (0.7 mg, 32%) was isolated (CH_2Cl_2/MeOH 40:1, R_f 0.36) and characterized.) **13b**: TLC (CH_2Cl_2/MeOH 40:1) R_f 0.28; UV−vis (CH_2Cl_2) 645 (8200), 589 (8300), 549 (12 800), 514 (29 200), 418 (690 000); ^{1}H NMR (400 MHz, $CDCl_3$) δ −2.64 (s, 2 H, exchange with D_2O), 1.02, 1.04 (d, 3 H), 1.17 (s, 3 H), 1.24 (s, 3 H), 1.29 (s, 9 H), 1.47−1.90, 1.95−2.14, 2.14−2.28, 2.30−2.44 (4m, ca. 26 H), 2.65−2.67 (m, 1 H), 2.95−3.14, 3.18−3.44, 3.50−3.62 (3m, ca. 13 H), 3.79−3.81 (m, 1 H), 3.84−3.89 (dd-lk m, 1 H) 3.91−3.97 (dd-lk m, 2 H), 4.02−4.12 (m, 2 H), 4.37−4.39 (d-lk m, 1 H), 4.71−4.74 (m, 1 H), 4.91−4.95 (m, 1 H) 5.09−5.13 (m, 1 H), 5.76−5.80 (m, 3 H), 5.91−5.94 (m, 1 H); 7.82−7.88 (2m, 18 H), 8.07−8.11 (m, 12 H), 8.27 (d, 4 H, J = 6.63 Hz), 8.40 (d, 4 H, J = 8.06 Hz), 8.76−8.86 (m, 16 H); ^{2}H NMR (46 MHz, $CHCl_3$): 5.53−5.65; FAB-MS *m/z* 1545 (100, M − **1** + 18 + H^+). **13c**: R_f 0.17, R_f 0.14; UV−vis (CH_2Cl_2) 645 (4400), 589 (4450), 549 (6900), 514 (15 700), 418 (371 000), 365 (sh, 31 500); ^{1}H NMR (400 MHz, $CDCl_3$). Due to the small amount and the product mixture the spectrum of **13c** only confirms the presence of porphyrin and BTX (1:1); FAB-MS *m/z* 1543 (M^+).

Acknowledgment. This work was supported by NIH GM 34509 (to K.N.), Schweizerischer Nationalfonds (to S.M.), NIH GM 22994 and NIH Fogarty Senior International Fellowship F06 TW02122 (to R.W.W.), and Deutsche Forschungsgemeinschaft Grant FI 142/3-2 (to J.F.).

JA960126P